ARTICLE

TLR9 agonist enhances radiofrequency ablation-induced CTL responses, leading to the potent inhibition of primary tumor growth and lung metastasis

Aizhang Xu[1,2], Lifeng Zhang[3], Jingying Yuan[1,2], Fatma Babikr[1,2], Andrew Freywald[4], Rajni Chibbar[4], Michael Moser[5], Wenjun Zhang[6], Bing Zhang[7], Zhaoying Fu[8] and Jim Xiang[1,2]

Radiofrequency ablation (RFA) is the most common approach to thermal ablation for cancer therapy. Unfortunately, its efficacy is limited by incomplete ablation, and further optimization of RFA is required. Here, we demonstrate that incubation at 65 °C triggers more EG7 tumor cell death by necrosis than treatment at 45 °C, and the 65 °C-treated cells are more effective at inducing antigen-specific $CD8^+$ cytotoxic T lymphocyte (CTL) responses after injection in mice than the 45 °C-treated ones. Dendritic cells (DCs) that phagocytose 65 °C-treated EG7 cells become mature with upregulated MHCII and CD80 expression and are capable of efficiently inducing effector CTLs in mouse tumor models. RFA (65 °C) therapy of EG7 tumors induces large areas of tumor necrosis and stimulates CTL responses. This leads to complete regression of small (~100 mm^3) tumors but fails to suppress the growth of larger (~350 mm^3) tumors. The administration of the Toll-like receptor-9 (TLR9) agonist unmethylated cytosine-phosphorothioate-guanine oligonucleotide (CpG) to DCs phagocytosing 65 °C-treated EG7 cells enhances the expression of MHCII and CD40 on DCs as well as DC-induced stimulation of CTL responses. Importantly, the intratumoral administration of CpG following RFA also increases the frequencies of tumor-associated immunogenic $CD11b^-CD11c^+CD103^+$ DC2 and $CD11b^+F4/80^+MHCII^+$ M1 macrophages and increases $CD4^+$ and $CD8^+$ T-cell tumor infiltration, leading to enhanced $CD4^+$ T cell-dependent CTL responses and potent inhibition of primary RFA-treated or distant untreated tumor growth as well as tumor lung metastasis in mice bearing larger tumors. Overall, our data indicate that CpG administration, which enhances RFA-induced CTL responses and ultimately potentiates the inhibition of primary tumor growth and lung metastasis, is a promising strategy for improving RFA treatment, which may assist in optimizing this important cancer therapy.

Keywords: TLR9 agonist; RFA; CTL response; antitumor immunity; metastasis

Cellular & Molecular Immunology (2019) 16:820–832; https://doi.org/10.1038/s41423-018-0184-y

INTRODUCTION

Radiofrequency ablation (RFA) is the most common approach to thermal ablation for cancer therapy.[1] In specific cancer cases, such as small liver tumor metastasis, RFA therapy produces clinical outcomes comparable to surgical resection.[2–4] Overall, RFA offers some significant advantages compared to surgical procedures, including lower morbidity, lower costs and better preservation of surrounding tissues.[5] However, its most common drawback is incomplete tumor ablation, leading to cancer recurrence.

$CD8^+$ cytotoxic T lymphocytes (CTLs) play an important role in host defense against tumors.[6] RFA-induced $CD8^+$ CTL responses were mostly observed in a nonspecific manner by assessing interferon-γ (IFN-γ)-positive staining of $CD8^+$ T cells by flow cytometry,[7] and antigen-specific responses were assessed by semiquantitative ELISPOT (Enzyme Linked Immuno Spot Assay) analysis in animal models[8] or in clinical trials.[9–11] The development of highly specific immune detection reagents using fluorescently labeled tetramer–major histocompatibility complex (MHC)–peptide complexes, such as phycoerythrin (PE)-labeled H-$2K^b/OVA_{257–264}$ tetramer (PE-Tetramer), has made it possible to quantitatively and qualitatively characterize ovalbumin antigen (OVA)-specific T cells by flow cytometry.[12]

In conjunction with some other reports,[13–15] we previously demonstrated that dendritic cells (DCs) that phagocytose apoptotic EG7 and $BL6–10_{OVA}$ tumor cells, which were both engineered to express OVA as a model tumor antigen, induced potent OVA-specific CTL responses detected by flow cytometry.[16,17] In addition, we have recently constructed and validated a custom-made RFA device capable of generating RFA-induced cell death in hepatoma tissue.[18,19] With minor modifications, this device is suitable for studying RFA-induced CTL responses in tumor models in vivo.

[1]Cancer Research, Saskatchewan Cancer Agency, University of Saskatchewan, Saskatoon, SK, Canada; [2]Department of Oncology, University of Saskatchewan, Saskatoon, SK, Canada; [3]Department of General Surgery, The First Affiliated Hospital of Soochow University, Suzhou, China; [4]Department of Pathology, University of Saskatchewan, Saskatoon, SK, Canada; [5]Department of Surgery, University of Saskatchewan, Saskatoon, SK, Canada; [6]Department of Bioengineering, University of Saskatchewan, Saskatoon, SK, Canada; [7]Biomedical Science and Technology Research Center, School of Mechatronic Engineering and Automation, Shanghai University, Shanghai, China and [8]Department of Immunology, College of Medicine, Yian-An University, Yian-An, China
Correspondence: Jim Xiang (jim.xiang@usask.ca)

Received: 29 August 2018 Accepted: 25 October 2018
Published online: 22 November 2018

In this study, we performed in vitro heat (45 °C and 65 °C) treatment of mouse EG7 thymoma cells expressing OVA on the cell surface, followed by assessment of the heat shock-induced effect on cell death. A temperature of 65 °C was selected because protein denaturation and cell death have been shown to occur above 55 °C.[20] We generated DCs that phagocytosed the heat-treated EG7 tumor cells and assessed their immunogenicity in C57BL/6 mice. We also assessed OVA-specific CTL responses and monitored tumor growth in mice bearing subcutaneous (s.c.) EG7 tumor post RFA. We showed that DCs that phagocytosed 65 °C-treated EG7 cells became mature DCs with upregulated MHCII and CD80 expression. These cells stimulated stronger CTL responses compared to DCs that phagocytosed 45 °C-treated EG7 cells. In vivo RFA (65 °C) therapy of EG7 tumors induced tumor necrosis and stimulated CTL responses, leading to complete regression of small EG7 tumors, but failed to inhibit larger EG7 tumor growth in C57BL/6 mice. To improve the therapeutic effect, we administered immune adjuvants, such as the Toll-like receptor-9 (TLR9) agonist CpG.[21,22] We found that the administration of CpG to DCs actively phagocytosing 65 °C-treated EG7 cells significantly enhanced DC expression of MHCII, CD40 and CD80 and strengthened the stimulation of CTL responses. Our investigation also revealed that the intratumoral administration of CpG post RFA increased the frequencies of tumor-associated immunogenic $CD11b^{-}CD11c^{+}CD103^{+}$ type 2 DCs (DC2) and $CD11b^{+}F4/80^{+}MHCII^{+}$ type 1 (M1) macrophages and enhanced T-cell tumor infiltration, leading to enhanced $CD4^{+}$ T cell-dependent CTL responses and potent inhibition of primary RFA-treated or distant untreated tumor growth and lung metastasis in mice bearing larger (~350 mm^3) EG7 tumors. Therefore, our data unambiguously suggest that the TLR9 agonist enhances RFA-induced CTL responses, leading to potent inhibition of primary tumor growth and distant metastasis.

MATERIALS AND METHODS

Reagents, cell lines and mice

Chicken OVA and a mouse monoclonal anti-OVA antibody (OVA-14) were obtained from Sigma-Aldrich Canada Ltd. (Oakville, Ontario, Canada). EG7 cells, an OVA transgene-transfected mouse thymoma cell line obtained from American Type Culture Collection (ATCC, Rockville, MD), was maintained in Dulbecco's-modified Eagle's medium (DMEM) (Life Technologies, Carlsbad, CA) supplemented with 10% fetal calf serum (FCS) and G418 (0.5 mg/mL; Life Technologies). BL6–10_{OVA} cells are an OVA transgene-transfected BL6–10 melanoma cell line with a high potential for lung metastasis.[16] EG7 and BL6–10_{OVA} cells were maintained in complete minimum essential medium-alpha containing 10% FCS and G418 (0.5 mg/mL). A PE-labeled H-$2K^b$/$OVA_{257–264}$ tetramer (PE-Tetramer) and fluorescein isothiocyanate (FITC)-labeled anti-CD8 antibody were obtained from Beckman Coulter (San Diego, CA). Anti-CD45-PE, anti-CD11c-PECy5, anti-CD11b-APC, anti-I-A/I-E-APC-Cy7 (MHCII), anti-$CD103^{-}$BV421, anti-F4/80-PECy5, anti-CD206-BV421, anti-CD8-PE and anti-CD45.1-APC antibodies; biotin-labeled antibodies specific for CD11c, CD11b, CD40, CD80, CD103 and MHCII; FITC- or PE-labeled secondary antibodies; appropriate isotype-matched control antibodies; and a Zombie Aqua Fixable Viability Kit were obtained from Biolegend (San Diego, CA). A Tumor Dissociation Kit was purchased from Miltenyi (San Diego, CA). Anti-CD4, anti-CD8 and anti-NK1.1 antibodies were obtained from Biolegend. CpG (ODN 1826) was purchased from InvivoGen Inc. (San Diego, CA). A FITC-Annexin V Apoptosis Detection Kit was purchased from BD Pharmingen Canada Inc. (Mississauga, Ontario, Canada). All cytokines were purchased from Peprotech (Rocky Hill, NJ). Female C57BL/6 (B6, CD45.2), B6.1 (CD45.1) and OVA-specific TCR transgenic OT-I mice were purchased from Jackson Laboratory (Bar Harbor, MA). CD45.1-OT-I mice were obtained by cross-breeding B6.1 mice with OT-I mice. All animal experiments were performed according to protocols and guidelines approved by the Animal Research Ethics Board, University of Saskatchewan.

Dendritic cell preparation

C57BL/6 mouse bone marrow-derived DCs were prepared as described previously.[23] Briefly, bone marrow cells from the tibia and femur of naive C57BL/6 mice were depleted of red blood cells with 0.84% Tris-ammonium chloride and cultured in DC culture medium (DMEM plus 10% FCS, granulocyte macrophage colony stimulation factor (GM-CSF) (20 ng/mL), and interleukin (IL)−4 (20 ng/mL)). On day 3, the nonadherent granulocytes and B and T cells were gently removed, and fresh medium was added. On day 6, released, mature and nonadherent cells with the typical morphologic features of DCs were harvested. DCs were analyzed for the expression of a DC marker (CD11c) and DC maturation markers (MHCII, CD40 and CD80) using a flow cytometer. Sample data were acquired on a Cytoflex (Beckman Coulter, Brea, CA) and analyzed with FlowJo software (TreeStar, San Diego, CA). To boost OVA-specific memory T-cell responses, DCs were incubated with OVA (1 mg/mL) in culture medium overnight and termed DC_{OVA}.[23]

Preparation and characterization of heat-treated EG7 cells

EG7 cells were resuspended in complete medium at 10×10^6 cells/mL. Culture tubes were submerged in a water bath and incubated at 45 °C or 65 °C for 5 min, which was the optimal exposure time for maximal heat-induced cell death at 45 °C or 65 °C (data not shown). Control and heat-treated cells were characterized immediately after heating by staining the cells with FITC-labeled anti-Annexin V antibody and propidium (PI) or FITC-labeled anti-HSP70 antibody and assessing the cells with flow cytometry and confocal microscopy analyses. Tumor cells stained only by Annexin V (early apoptosis marker) and those costained by Annexin V and PI (late apoptosis or necrosis marker) represent the early apoptotic and late apoptotic cells, respectively. To assess immunogenicity, heat-treated EG7 cells (1×10^6 cells/mouse) were intravenously (i.v.) injected into mice. Mouse tail blood samples were harvested 7 days post cell injection, stained with a FITC-labeled anti-CD8 antibody and PE-tetramer and analyzed by flow cytometry.

Generation and characterization of DCs that phagocytose heat-treated tumor cells

Heat-treated tumor cells were resuspended in posphate-buffered saline (PBS) at 1×10^7 cells/ml and incubated with carboxyfluorescein succinimidyl ester (CFSE) (4 μM) at 37 °C for 10 min. The labeled cells were washed 3 times with PBS. DCs were cultured with CFSE-labeled tumor cells at a ratio of 1:2 in culture medium containing GM-CSF (10 ng/mL) at 37 °C overnight. The overnight culture mixtures were harvested. Live cells were purified with Ficoll-Paque gradient centrifugation, stained with a PE-labeled anti-CD11c antibody (red) for cell surface CD11c molecules and 4′,6-diamidino-2-phenylindole (DAPI; blue) for nuclei and then analyzed by flow cytometry and confocal microscopy according to a protocol we previously described.[17] Alternatively, DCs were fixed with 4% paraformaldehyde for electron microscopy to visualize DC phagocytosis according to a protocol we previously reported.[16] To assess the immunogenicity of the DCs, we prepared DCs that phagocytosed heat-treated tumor cells during the overnight incubation of the DCs with the 45 °C-treated and 65 °C-treated tumor cells at a ratio of 1:2 in the absence or presence of CpG (10 μg/mL). These cells were termed $DC_{EG7(45C)}$ and $DC_{EG7(65C)}$ or $DC_{EG7(65C)/CpG}$ according to the incubation conditions.

RFA treatment

EG7 cells (4×10^6 cells/mouse) were s.c. injected into the right flank of C57BL/6 mice. Tumor growth was monitored. Tumors gradually grew and often reached ~100 mm^3 (~6 mm in

diameter, small size tumor) and ~350 mm^3 (~9 mm in diameter, large size tumor) 8–10 and 14–16 days, respectively, after tumor cell challenge. When tumors reached ~100 mm^3 or ~350 mm^3 in size, the mice (6–8 mice per group) were anesthetized with inhaled isoflurane gas (5% isoflurane for anesthesia induction; 2% for maintenance) and positioned on an electricity-conducting grounding pad wetted with distilled water prior to RFA. RFA (65 °C) was then performed using a custom-built 17-gauge single ablation electrode with a 0.5 cm active tip[24] inserted into the center of the tumor. The apparatus allowed the tumor tissue to reach the goal temperature (65 °C) in less than a minute in each case and maintained a constant temperature for the entire length of the treatment via a feedback loop. RFA (65 °C) treatment was administered for 5 min at the goal temperature for each mouse. The mice recovered on a warming blanket and were given a s.c. injection of an analgesic (buprenorphine 0.05 mg/kg body weight) for pain control. For CpG adjuvant administration, mice were intratumorally injected with 10 μg of CpG in 30 μL PBS (three injections of 10 μL each to tumor peripheral areas) after RFA treatment. To assess the involvement of $CD4^+$ or $CD8^+$ T cells or natural killer (NK) cells in RFA- or RFA/CpG-induced antitumor immunity, tumor-bearing mice were intraperitoneally injected with anti-CD4, anti-CD8, anti-NK1.1 or control antibodies (300 μg/mouse, 1 day prior to RFA and then once every 3 days for a total of 4 injections) for $CD4^+$ T cell, $CD8^+$ T cell, NK cell and control depletions, respectively.[25] To examine whether local RFA treatment could decrease the growth of distant tumors, C57BL/6 mice were injected subcutaneously with EG7 cells (4×10^6 and 2×10^6) on the right and left sides of the lower back, respectively. When the right and left tumors reached ~350 mm^3 and ~200 mm^3, respectively, RFA +CpG or RFA treatment was performed only on the right tumor. The mice were monitored for tumor growth at both the RFA-treated (right) and distant untreated (left) sites. Tumor volumes were calculated using the formula: tumor volume = $width^2 \times length/2$.[26] For ethical reasons, mice bearing ~2500 mm^3 tumors (with a diameter of ~20 mm) were killed and recorded as mouse death. To assess whether RFA-induced CTL responses could protect mice from tumor lung metastasis, C57BL/6 mice bearing larger tumors (5 mice per group) were i.v. injected with $BL6\text{–}10_{OVA}$ (0.5×10^6 cells/mouse), and RFA or RFA+CpG was performed 1 day later. Subcutaneous EG7 tumors were surgically removed 7 days post RFA. Mouse lungs were collected 20 days after $BL6\text{–}10_{OVA}$ injection. Black tumor colonies in the lungs were counted and confirmed by histological examination. To assess the OVA-specific $CD8^+$ T cell memory response derived from RFA-induced OVA-specific CTL responses, RFA-treated tumors were surgically removed 7 days post RFA, and the mice were given an i.v. boost with DC_{OVA} (1×10^6 cells/mouse) 25 days post RFA. Memory $CD8^+$ T-cell recall responses were analyzed in tail blood samples from boosted mice by flow cytometry 4 days after the boost.[25]

Assessment of OVA-specific CTL responses

To monitor OVA-specific CTL responses, mouse tail blood samples from DC (with phagocytosis of heat-treated tumor cells)-immunized or RFA-treated C57BL/6 mice were stained with PE-Tetramer and a FITC-labeled anti-CD8 antibody and analyzed by flow cytometry. The in vivo CTL cytotoxicity assay was performed in RFA (65 °C)-treated mice by transferring both $OVA_{257–264}$ peptide-pulsed CFSE (3.0 μM)-labeled ($CFSE^{high}$) and control irrelevant Mut1 peptide-pulsed CFSE (0.6 μM)-labeled ($CFSE^{low}$) target splenocytes at a ratio of 1:1 (each 10×10^6 cells). The $CFSE^{high}$ (H) and $CFSE^{low}$ (L) target cells remaining in the recipients' spleens were analyzed by flow cytometry 16 h later as previously described.[27] Sample data were acquired on a FACSCalibur (BD Bioscience) and analyzed with FlowJo software (TreeStar, San Diego, CA).

Assessment and characterization of tumor-associated DCs and macrophages and tumor-infiltrating T cells

EG7 cells were originally derived from the C57BL/6 mouse lymphoma cell line EL4, which expresses leukocyte common antigen CD45.2 (data not shown). To assess the tumor-infiltrating immune cells, B6.1 mice (CD45.1) were challenged with EG7 cells. Tumor tissue samples derived from EG7 tumors were used to prepare single cell suspensions (SCSs) by cutting the tissue samples into 1 mm^3 fragments in 5 mL of PBS containing 100 U/mL of collagenase IV and 1 mg/mL of DNase-I and incubating the mixture at 37 °C for 30 min, followed by the homogenization of the mixture with a syringe plunger. Tumor SCSs were filtered through a 40 μm filter. Erythrocytes were lysed by incubation of the SCSs for 5 min with red blood cell lysis buffer (PBS containing 0.15 M NH_4Cl, 10 mM $KHCO_3$ and 0.1 mM EDTA). Cells in tumor SCSs were stained with various antibodies to assess the amounts of intratumoral tolerogenic $CD11b^+CD11c^+CD103^-$ type 1 DCs (DC1), immunogenic $CD11b^-CD11c^+CD103^+$ type 2 DCs (DC2)[28] and inflammatory $CD11b^+F4/80^+MHCII^+$ type 1 macrophages (macrophage-1 or M1) or tolerogenic $CD11b^+F4/80^+MHCII^-$ type 2 macrophages (macrophage-2 or M2)[29] as well as intratumoral $CD4^+$ and $CD8^+$ T cells. Dead cells were excluded using the Zombie Aqua Fixable Viability dye (Biolegend). Data were collected on a CytoFLEX (Beckman Coulter) cytometer and analyzed using FlowJo software (TreeStar).

T-cell proliferation assays

For the in vitro T-cell proliferation assay, EG7 tumor-bearing mice were first treated with RFA or RFA+CpG as indicated above. After 2 days, DCs were purified from tumor-draining lymph nodes using a biotin-labeled anti-CD11c antibody and anti-biotin microbeads. Naive $CD8^+$ T cells purified from B6.1/OT-I mice using a CD8 T Cell Isolation kit (Stem cells Inc.) were labeled with CFSE (4 μM) and incubated with lymph node-derived DCs that had been irradiated with 2000 rad at a ratio of 1:1 in the presence of IL-2 (40 U/mL) and beta-mercaptoethanol (50 μM). After 3 days of incubation, activated $CD8^+$ T cells were stained with a PE-labeled anti-CD8 antibody and analyzed to show T-cell divisions by flow cytometry. For the in vivo T-cell proliferation assay, naive $CD8^+$ T cells purified from B6.1/OT-I mice were labeled with CFSE (4 μM) and i.v. transferred (5×10^6 cells/mouse) into EG7 tumor-bearing mice. RFA treatment was performed 16 h later. At 4 days after RFA (65 °C) treatment, the mouse tail blood samples were stained with anti-CD45.1-APC and anti-CD8-PE antibodies and analyzed by flow cytometry. CD45.1- and CD8 double-positive cells were gated for the analysis of T-cell divisions. Sample data were acquired on a cytometer and analyzed using FlowJo software.

Statistical analysis

Data represent the mean ± standard derivation. Student's *t*-test was applied to compare the variables from different groups.[17] A value of $p < 0.05$ was considered statistically significant.

RESULTS

Tumor cells undergoing hyperthermia-induced necrosis are immunogenic

A temperature of 65 °C was selected for our experiments due to the knowledge that protein denaturation and cell death have been shown to occur at temperatures above 55 °C.[20] To assess the effect of different temperatures on tumor cell death, we treated OVA-expressing EG7 tumor cells (Fig. 1a) in vitro at 45 °C and 65 °C for 5 min, followed by staining these cells with an anti-Annexin V antibody (early apoptosis marker) and PI (Annexin V/PI double staining indicates necrosis) or with an anti-HSP70 (necrosis marker) antibody. The stained cells were analyzed by flow cytometry. This experiment demonstrated that significant proportions of the heat-treated tumor cells stained positive for both

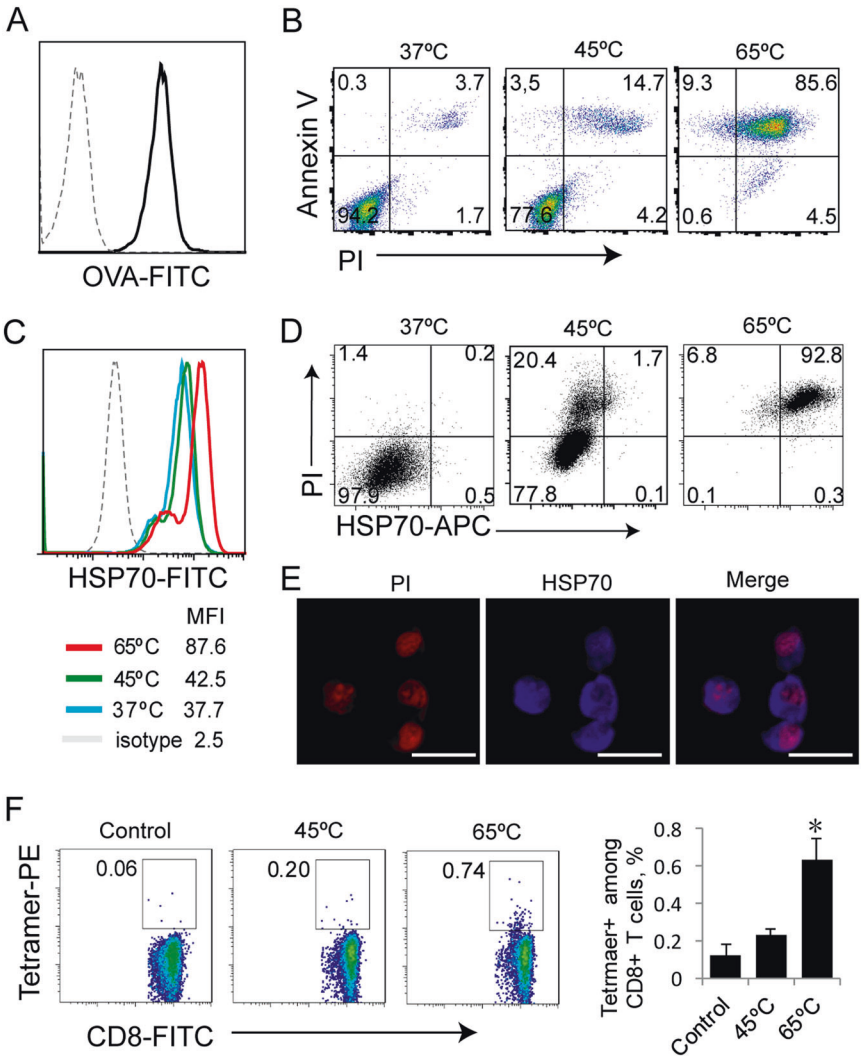

Fig. 1 Hyperthermia-treated apoptotic tumor cells are immunogenic. **a** EG7 cells were stained with an anti-OVA (dark line) or isotype control antibody (dotted line) and assessed by flow cytometry. **b** Heat (45 °C and 65 °C)-treated and control EG7 cells were stained with FITC-labeled anti-Annexin V antibody and PI and analyzed by flow cytometry. The gating for necrotic cells (45 °C and 65 °C) expressing Annexin V and PI was based upon the assessment of the live cells (37 °C). **c** Heat-treated EG7 cells were stained with an anti-HSP70 antibody (color lines) or isotype control antibody (dotted line) and analyzed by flow cytometry. Mean fluorescence intensity (MFI) numbers are indicated. **d** Heat-treated EG7 cells were stained with PI and an anti-HSP70 Ab and analyzed by flow cytometry. The gating for necrotic cells (45 °C and 65 °C) expressing both intracellular PI and intracellular HSP70 was based upon the assessment of the live cells (37 °C). The value in the right upper quadrant represents the percentage of apoptotic cells expressing HSP70. **e** Representative fluorescence images of heat-treated EG7 cells that were stained with PI and an anti-HSP70 Ab are shown. **f** Heat-treated EG7 tumor cells (1×10^6 cells/mouse) were i.v. injected into mice (6 per group). At 7 days after the cell injection, blood samples from immunized mice were stained with OVA-specific PE-Tetramer and a FITC-labeled anti-CD8 antibody and analyzed by flow cytometry. The gating for OVA-specific CTLs stained with both FITC-labeled anti-CD8 antibody and PE-tetramer in mice immunized with heat (45 °C and 65 °C)-treated EG7 tumor cells was based upon the assessment of CTLs in the control PBS-treated mice. A total of 20,000 $CD8^+$ T cells were counted. The value in each panel represents the percentage of OVA-specific $CD8^+$ T cells among the total $CD8^+$ T-cell population. $^*P < 0.05$ versus the cohort of $CD8^+$ T cells activated by 45 °C-treated EG7 (Student's *t* test). One representative experiment out of two total experiments is shown

Annexin V and PI, indicating that the tumor cells become necrotic (Fig. 1b). Heat treatment at a higher temperature (65 °C) induced a stronger apoptotic response (85%) than (14%) heat treatment at a lower temperature (45 °C) (Fig. 1b). In addition, we also found that 65 °C-treated tumor cells expressed higher levels of heat shock protein-70 (HSP70) than 45 °C-treated cells (Fig. 1c) and that HSP70 expression was correlated with cell death by flow cytometry (Fig. 1d), and enhanced HSP70 expression was intracellularly detected by confocal microscopy (Fig. 1e). To assess the immunogenicity of the necrotic tumor cells, we i.v. immunized C57BL/6 mice with the heat-treated tumor cells. At 7 days post immunization, mouse blood samples were collected, and cells were stained with a FITC-labeled anti-CD8 antibody and PE-Tetramer and analyzed by flow cytometry. The analysis demonstrated that the 65 °C-treated EG7 cells stimulated stronger OVA-specific $CD8^+$ T-cell responses (0.74%) than the 45 °C-treated cells (0.20%) (Fig. 1f), indicating that in vitro 65 °C-treated tumor cells are more immunogenic.

DCs that phagocytose 65 °C-treated tumor cells develop a mature DC phenotype

We allowed DCs to phagocytose necrotic tumor cells by coculturing DCs with heat-treated tumor cells overnight. To visualize phagocytosis, we performed electron microscopy. We demonstrated that necrotic EG7 cells with collapsed nuclei were phagocytosed by DCs (Fig. 2a). Alternatively, EG7 tumor cells

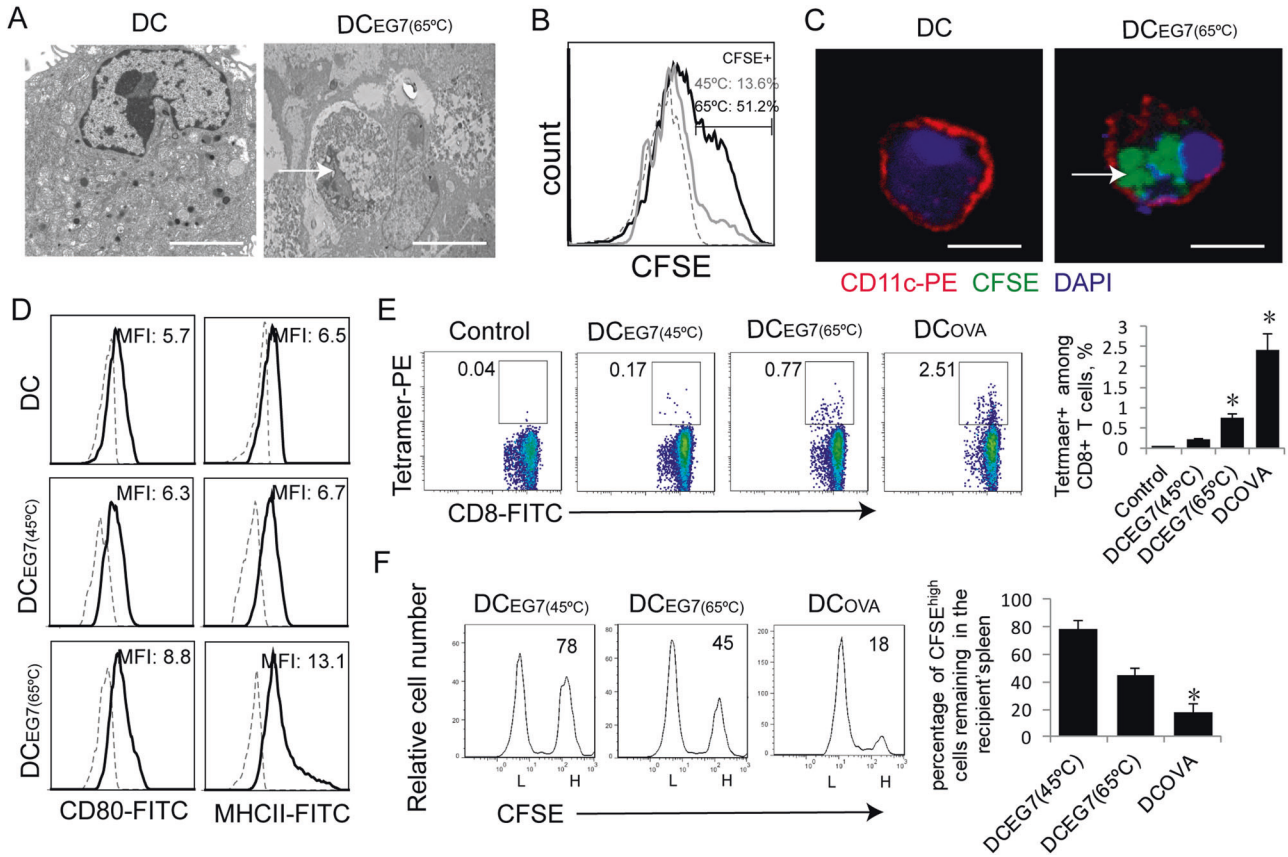

Fig. 2 DCs that phagocytose hyperthermia-treated tumor cells stimulate $CD8^+$ CTL responses. **a** Electron microscopy images of an untreated DC and a DC with a phagocytosed necrotic EG7 tumor cell (arrow) within its cytoplasm. Scale bar = 10 μm. **b** Flow cytometry histogram showing the fluorescence intensity of control DCs (dotted line) and DCs containing phagocytosed CFSE-labeled 45 °C-treated (gray line) or 65 °C-treated EG7 cells (dark line). **c** Representative confocal images showing CFSE (green)-labeled 65 °C-treated EG7 cells (arrow) phagocytosed into the cytoplasm of PE (red)-labeled CD11c-positive DCs. Scale bar = 20 μm. **d** Purified DCs were stained with anti-CD80, anti-Ia^b (solid lines) and isotype control Abs (dotted line) and analyzed by flow cytometry. Mean fluorescence intensity (MFI) numbers are indicated. **e** Cells in blood samples from mice (4 each group) immunized with DCs that phagocytosed heat-treated EG7 cells were stained with OVA-specific PE-Tetramer and a FITC-labeled anti-CD8 antibody and analyzed by flow cytometry. The gating for OVA-specific CTLs stained with both the FITC-labeled anti-CD8 antibody and PE-tetramer from mice immunized with $DC_{EG7\ (45\ °C)}$ and $DC_{EG7\ (65\ °C)}$ was based on the assessment of CTLs in the control PBS-treated mice. A total of 20,000 $CD8^+$ T cells were counted. The value in each panel represents the percentage of OVA-specific $CD8^+$ T cells among the total $CD8^+$ T-cell population. *$P < 0.05$ versus cohort of $DC_{EG7(45\ °C)}$-activated $CD8^+$ T cells (Student's *t*-test). **f** In vivo cytotoxicity assay. The OVA-specific $CFSE^{high}$ (H) and control $CFSE^{low}$ (L) target cells remaining in the spleen of mice (4 each group) immunized with $DC_{EG7(45\ °C)}$ and $DC_{EG7(45\ °C)}$ were analyzed by flow cytometry. The value in each panel represents the percentage of $CFSE^{high}$ target cells remaining in the recipient's spleen. *$P < 0.05$ versus the cohort of $DC_{EG7(45\ °C)}$-immunized mice (Student's *t*-test). One representative experiment out of two experiments is shown

initially labeled with the fluorescent dye CFSE (green) were treated with heat, and these heat-treated CFSE-labeled EG7 tumor cells were cocultured with DCs. In this approach, DC phagocytosis of CFSE-labeled necrotic EG7 cells was confirmed by flow cytometry (Fig. 2b) and confocal microscopy analyses (Fig. 2c). $CFSE^+$ DCs were found to be more frequent in $DC_{EG7(65C)}$ cultures (51.2%) than in $DC_{EG7(45C)}$ cultures (13.6%) ((Fig. 2b). To assess phenotypic changes in DCs, we also performed a flow cytometry analysis. We observed that DCs that phagocytosed 65 °C-treated EG7 tumor cells displayed higher expression of MHCII and CD80 than DCs that phagocytosed 45 °C-treated EG7 tumor cells (Fig. 2d), indicating that the DCs that phagocytosed 65 °C-treated EG7 tumor cells have a more mature phenotype.

DCs that phagocytose 65 °C-treated tumor cells stimulate more efficient CTL responses

We i.v. immunized mice with OVA-presenting DC_{OVA} and DCs that phagocytosed heat (65 °C or 45 °C)-treated EG7 tumor cells ($DC_{EG7\ (65C)}$ or $DC_{EG7(45C)}$) and assessed OVA-specific $CD8^+$ T-cell responses 6 days post immunization. We demonstrated that vaccination of mice with the positive control DC_{OVA} efficiently induced OVA-specific $CD8^+$ T-cell responses (2.5%) (Fig. 2e). We found that $DC_{EG7(65C)}$ (0.77%) stimulated stronger OVA-specific $CD8^+$ T-cell responses than $DC_{EG7(45C)}$ (0.17%) (Fig. 2e), indicating that the $DC_{EG7(65C)}$ cells are more immunogenic in vivo. To assess the effector functions of stimulated OVA-specific $CD8^+$ T cells, we performed an in vivo cytotoxicity assay by adoptively transferring $OVA_{257–264}$ peptide-pulsed splenocytes that had been labeled with higher concentrations of CFSE ($CFSE^{high}$) and control peptide-pulsed splenocytes that had been labeled with lower concentrations of CFSE ($CFSE^{low}$) into the immunized mice. We then assessed the loss of the OVA-specific $CFSE^{high}$ target cells from the mouse splenocyte population by flow cytometric analysis. We found that 82% of $CFSE^{high}$ target cells disappeared in the 16 h after target cell transfer in the DC_{OVA}-immunized mice and that 55% of $CFSE^{high}$ target cells disappeared in the 16 h after target cell transfer in the $DC_{EG7(65C)}$-immunized mice, which is significantly more than that in the $DC_{EG7(45C)}$-immunized mice (22%) (Fig. 2f). This indicates that $DC_{EG7(65C)}$ induces a large number of OVA-specific effector CTLs with cytolytic activity. Therefore, we

selected RFA at a treatment temperature of 65 °C to further assess RFA-induced antitumor immunity.

RFA induces tumor necrosis, CTL responses and antitumor immunity

We first s.c. injected C57BL/6 mice with EG7 tumor cells and performed in vivo RFA (65 °C) when tumors reached small (~100 mm^3) or larger (~350 mm^3) sizes (Fig. 3a) using a previously constructed custom-made RFA device set to maintain a constant treatment temperature[18,19] for the administration of RFA in small animal models. To assess RFA-induced tumor cell death in larger tumors, we removed tumors 2 days after RFA for histopathologic examination. We demonstrated that compared with the control treatment, RFA (65 °C) induced a larger area of tumor necrosis 2 days post RFA (Fig. 3b) and significant tumor shrinkage at the center of the tumor 7 days post RFA (Fig. 3c). To assess RFA-induced $CD8^+$ T-cell responses, mouse blood samples were collected 7 days post RFA, and the cells were stained with a FITC-labeled anti-CD8 antibody and PE-Tetramer and analyzed by flow cytometry. This experiment showed that RFA (65 °C) treatment induced OVA-specific $CD8^+$ T-cell responses (0.63%) (Fig. 3d). To analyze RFA-induced antitumor immunity, we monitored tumor growth daily post RFA (65 °C) in animals with small tumors. We found that a single RFA (65 °C) treatment resulted in the complete eradication of small tumors in all 5 mice (Fig. 3e). This observation was confirmed by histological examination of tumor tissue sections, which showed that the small tumors (Fig. 3f) were replaced with scar tissue post RFA (Fig. 3g).

Intratumoral TLR9 agonist treatment increases tumor-associated immunogenic $CD11c^+CD103^+$ DC2 and enhances the stimulatory effect of $CD11c^+$ DCs on T-cell proliferation

Intratumoral tumor-associated DCs have recently been divided into two subsets: tolerogenic $CD11b^+CD11c^+CD103^-$ DC1 and immunogenic $CD11b^-CD11c^+CD103^+$ DC2.[30] The TLR9 agonist CpG is an immune adjuvant that increases vaccine immunogenicity by enhancing DC maturation and cytokine secretion.[21,22] To assess the effect of CpG on tumor-associated DCs in vivo, we intratumorally administered CpG and examined tumor-associated DCs by flow cytometry at day 2 post RFA, a time point when skin DCs are highly mobilized after protein immunization.[31] To dissect the tumor-associated DC populations, we devised a seven-color flow cytometry panel and progressive gating strategy using the EG7 (CD45.2) model established in B6.1 mice (CD45.1). Tumor-infiltrating leukocyte populations gated as $CD45.1^+$ were profiled. Neutrophils and monocytes were removed by subgating all the $CD45.1^+$ cells.[28] DCs identified as $CD11c^+MHC^+$ were found to separate into two populations based on the differential expression of CD11b and CD103. We showed an increased amount of immunogenic $CD11b^-CD11c^+CD103^+$ DC2 in the RFA+CpG-treated tumors compared to the RFA-treated or untreated tumors (Fig. 4a, b). To measure the stimulatory capacity of DCs derived from the RFA+CpG-treated or RFA-treated EG7 tumors, we cocultured the purified CFSE-labeled OT-I $CD8^+$ T cells with $CD11c^+$ DCs ($DC_{RFA+CpG}$, DC_{RFA} and $DC_{control}$) purified from the total splenocytes of the RFA+CpG-treated, RFA-treated and untreated EG7 tumor-bearing mice 1 day post RFA and analyzed the cultures by flow cytometry analysis after 3 days of in vitro culture. We demonstrated that the in vitro stimulatory effect of $DC_{RFA+CpG}$ (containing more DC2 than the DC_{RFA} sample) on T-cell proliferation is much stronger than that of DC_{RFA} (Fig. 4c). To assess intratumoral DC in vivo stimulatory effect, we i.v. injected CFSE-labeled OT-I $CD8^+$ T cells into EG7 tumor-bearing mice and assessed the proliferation of CFSE-labeled T cells derived from EG7 tumors with or without CpG injection 4 days post RFA (65 °C) treatment. We demonstrated that 32.9% of CFSE-labeled OT-I $CD8^+$ T cells injected into the RFA/CpG-treated tumors divided more than 3 times, while only 6.6% of CFSE-labeled OT-I $CD8^+$ T cells divided more than 3 times in the RFA-treated tumors (Fig. 4d).

Intratumoral TLR9 agonist administration increases the frequency of tumor-associated immunogenic $CD11b^+F4/80^+MHCII^+$ M1 and enhances $CD4^+$ and $CD8^+$ T-cell tumor infiltration

Intratumoral tumor-associated macrophages have been divided into two subsets: inflammatory $CD11b^+F4/80^+MHCII^+$ type 1 macrophages (M1) and tolerogenic $CD11b^+F4/80^+MHCII^-$ type 2 macrophages (M2).[29] To assess the effect of CpG on intratumoral macrophages in vivo, we intratumorally administered CpG and examined intratumoral macrophages by flow cytometry 2 days post RFA. To dissect the tumor-associated macrophage populations, we employed a seven-color flow cytometry panel and a progressive gating strategy using the EG7 model established in B6.1 mice. Macrophages gated as $CD11b^+F4/80^+$ within the $CD45.1^+$ cell population were found to separate into two populations based on the differential expression of MHCII, as observed in a colon adenoma model.[29] We demonstrated an increased amount of macrophages in the RFA+CpG-treated tumors compared to the RFA-treated or untreated tumors (Fig. 4e, f). We further showed an increased amount of inflammatory $CD11b^+F4/80^+MHCII^+$ M1 and reduced amount of tolerogenic $CD11b^+F4/80^+MHCII^-$ M2 in the RFA+CpG-treated tumors compared to the RFA-treated or untreated tumors (Fig. 4e, f). In addition, the RFA+CpG treatment also significantly enhanced $CD4^+$ T-cell tumor infiltration (2 days post treatment) and increased $CD4^+$ and $CD8^+$ T-cell tumor infiltration (6 days post treatment) compared with the RFA treatment (Fig. 4g).

Intratumoral TLR9 agonist enhances RFA-induced $CD4^+$ T cell-dependent CTL responses

To assess whether CpG improves RFA therapy, we intratumorally administered CpG after RFA (65 °C) treatment. CTL responses and effector functions were measured in these treated mice by flow cytometry analysis (Fig. 5a). We found that the intratumoral administration of CpG with RFA treatment significantly enhanced RFA-induced OVA-specific CTL responses (2.28%) compared to RFA treatment alone (0.82%) or CpG treatment alone (0.21%) (Fig. 5b). We also demonstrated that 75% of OVA-specific $CFSE^{high}$ target cells disappeared in the 16 h after target cell transfer in the RFA+CpG-treated mice, which is significantly more than that observed in the RFA-treated mice (28%) (Fig. 5c). This indicates that the RFA+CpG treatment induces potent OVA-specific effector CTLs with cytolytic activity. To assess the involvement of $CD4^+$ T cells in RFA+CpG-induced CTL responses, we depleted $CD4^+$ T cells using an anti-CD4 antibody one day before the RFA+CpG therapy and assessed CTL responses 7 days post RFA+CpG therapy. We demonstrated that the RFA+CpG therapy efficiently induced OVA-specific CTL responses (2.99%) and that $CD4^+$ T-cell depletion resulted in a nearly two-third reduction in the magnitude of the RFA+CpG therapy-induced CTL responses (Fig. 5d), indicating that RFA+CpG-induced CTL responses are $CD4^+$ T-cell dependent.

Intratumoral TLR9 agonist enhances the RFA-induced inhibition of primary RFA-treated and distant untreated tumor growth and lung metastases and increases RFA-induced memory T-cell recall responses

To assess whether CpG improves RFA therapy, we intratumorally administered CpG after RFA, monitored tumor growth and found that the RFA+CpG treatment significantly inhibited tumor growth, whereas the RFA or CpG alone treatment did not show any beneficial effect on large tumors (Fig. 6a). To assess the involvement of $CD4^+$ and $CD8^+$ T cells and NK cells in the RFA+CpG-induced inhibition of tumor growth, we depleted $CD4^+$ and $CD8^+$ T cells and NK cells with anti-CD4, anti-CD8 and anti-NK1.1 antibodies, respectively, in the RFA+CpG-treated mouse group

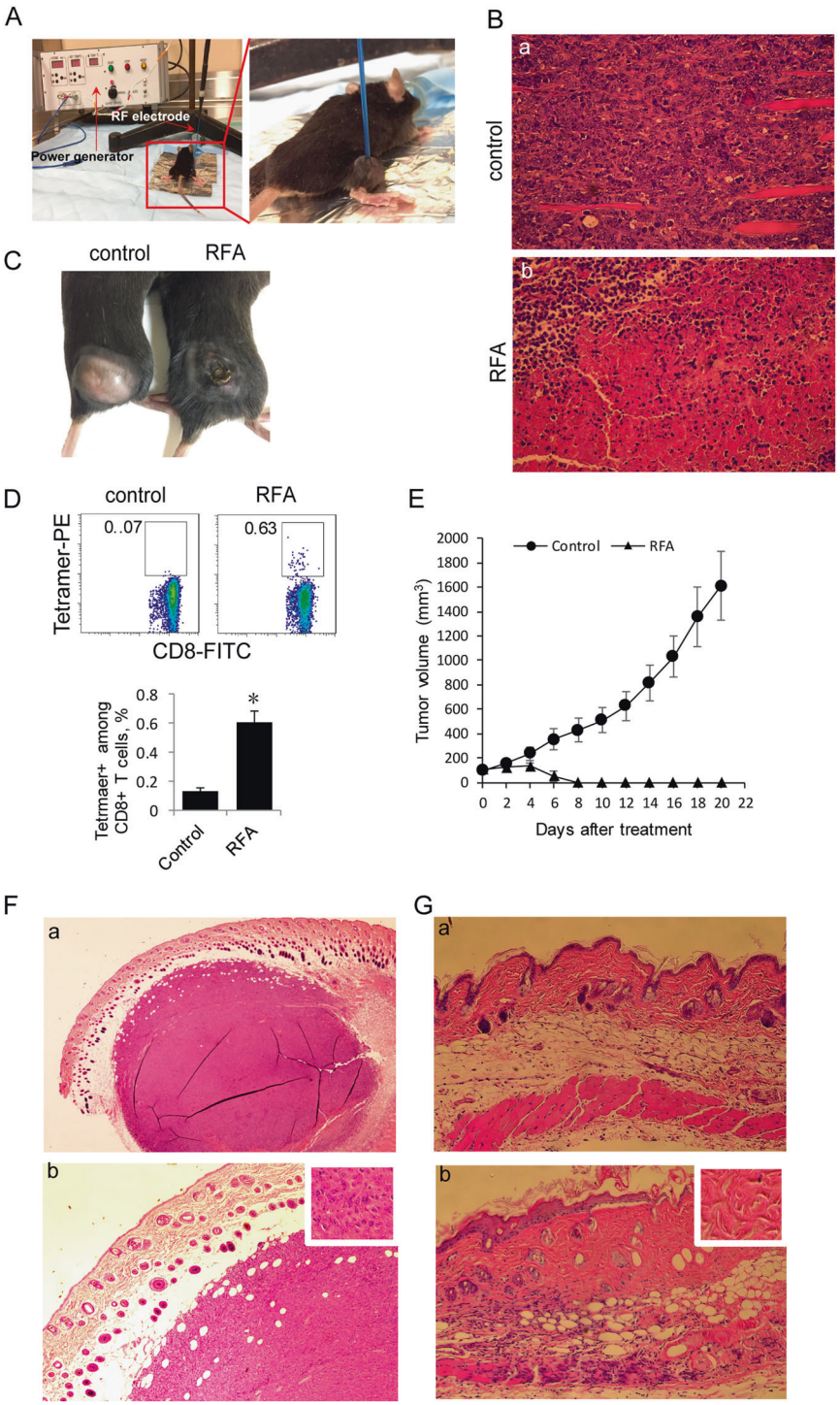

Fig. 3 RFA induces OVA-specific CD8$^+$ CTL responses and eliminates small tumors. **a** Experimental setup for RFA treatment. **b** Representative hematoxylin and eosin staining of tissue sections from a tumor collected 2 days post RFA treatment. Magnification, ×100. **c** Representative image showing the shrinkage of RFA-treated EG7 tumors in the center area where RFA was performed 7 days post RFA treatment. **d** Cells in blood samples from RFA-treated mice (4 each group) were stained with OVA-specific PE-Tetramer and a FITC-labeled anti-CD8 antibody and analyzed by flow cytometry. The gating for OVA-specific CTLs stained with both the FITC-labeled anti-CD8 antibody and PE-tetramer from tumor-bearing mice treated with RFA was based upon the assessment of CTLs in the control PBS-treated mice. A total of 20,000 CD8$^+$ T cells were counted. The value in each panel represents the percentage of OVA-specific CD8$^+$ T cells among the total CD8$^+$ T-cell population. The value in each parenthesis represents the standard deviation. *$P < 0.05$ versus the cohort of control mice (Student's *t*-test). **e** Tumor growth or regression was monitored post RFA treatment in RFA-treated and control mice (5 each group) bearing small EG7 tumors. **f** Representative hematoxylin and eosin staining of sections of a small tumor (~6 mm in diameter). Magnification, ×40 (a), 100 (b), and insert shows tumor tissue (×400). **g** Representative hematoxylin and eosin staining of sections of normal skin (a) and scar tissue (b) post RFA. Magnification, ×100. The insert shows scar tissue (×400). One representative experiment out of two total experiments is shown

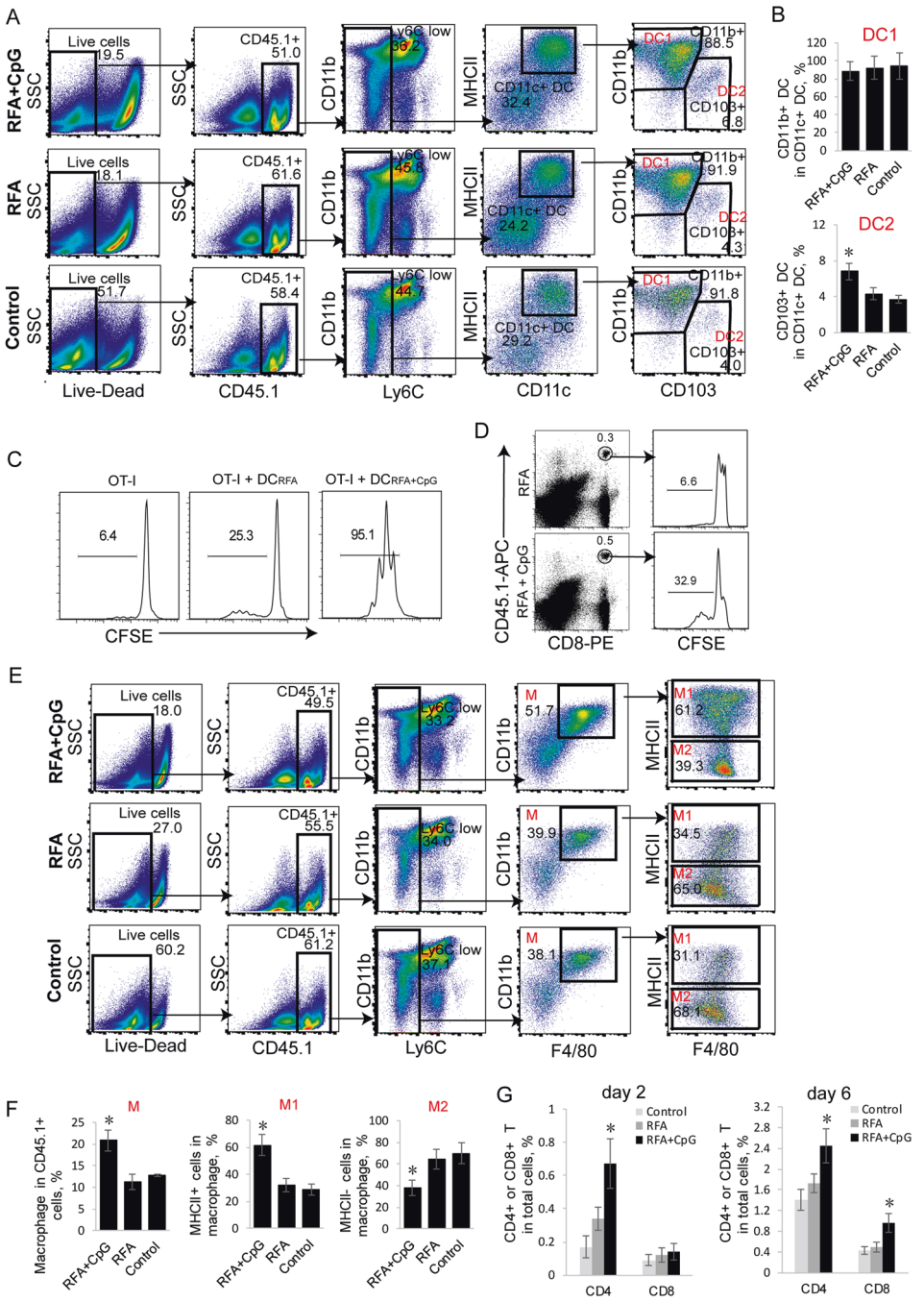

Fig. 4 Administration of adjuvant CpG increases the frequency of tumor-associated immunogenic DC2 and M1 and enhances T-cell tumor infiltration. **a**, **b** Flow cytometry analysis of tumor-associated DCs in tumor single cell suspensions derived from EG7 tumors in B6.1 mice was performed with a progressive gating strategy. The frequency of tumor-associated $CD11b^+CD11c^+$ DC1 and $CD11c^+CD103^+$ DC2 in the total $CD11c^+$ DC population at 2 days post treatment is shown; $n = 3$ mice per group. $^*P < 0.05$ versus the cohort of control mice (Student's *t*-test). **c** In vitro T-cell proliferation assay. Irradiated (2000 rad) DCs that had been initially purified from the tumor-draining lymph node cells of RFA– and RFA+ CpG-treated tumor-bearing mice were cultured with CFSE-labeled OT-I $CD8^+$ T cells for 3 days and analyzed for T-cell proliferation by flow cytometry. The value represents the percentage of cells that divided at least once. **d** In vivo T-cell proliferation assay. Cells from the tail blood samples of RFA- and RFA/CpG-treated EG7 tumor-bearing mice (4 each group) with transferred CFSE-labeled OT-I $CD8^+$ T cells were stained with anti-CD45.1-APC and anti-CD8-PE antibodies and analyzed by flow cytometry. CD45.1/CD8 double-positive T cells were gated for the analysis of T-cell proliferation. The value represents the percentage of cells that divided more than three times. **e**, **f** Flow cytometry analysis of tumor-associated macrophages from the tumor single cell suspensions derived from EG7 tumors in B6.1 mice by a progressive gating strategy. The frequency of tumor-associated $CD11b^+F4/80^+$ macrophages (M) in the total $CD45.1^+$ cell population as well as the frequency of tumor-associated inflammatory $CD11b^+F4/80^+Ia^{b+}$ M1 and tolerogenic $CD11b^+F4/80^+Ia^{b-}$ M2 in the total $CD11b^+F4/80^+$ M population at day 2 post treatment; $n = 3$ mice per group. $^*P < 0.05$ versus the cohort of control mice (Student's *t*-test). **g** The frequency of $CD4^+$ and $CD8^+$ T cells in the total cell population at day 2 and day 6 post treatment; $n = 5$ mice per group. Tumor-infiltrating T cells were gated from $CD45.1^+CD3^+$ cells and analyzed for the expression of CD4 and CD8 by flow cytometry. $^*P < 0.05$ versus the cohort of control RFA mice (Student's *t*-test). One representative experiment out of two experiments is shown

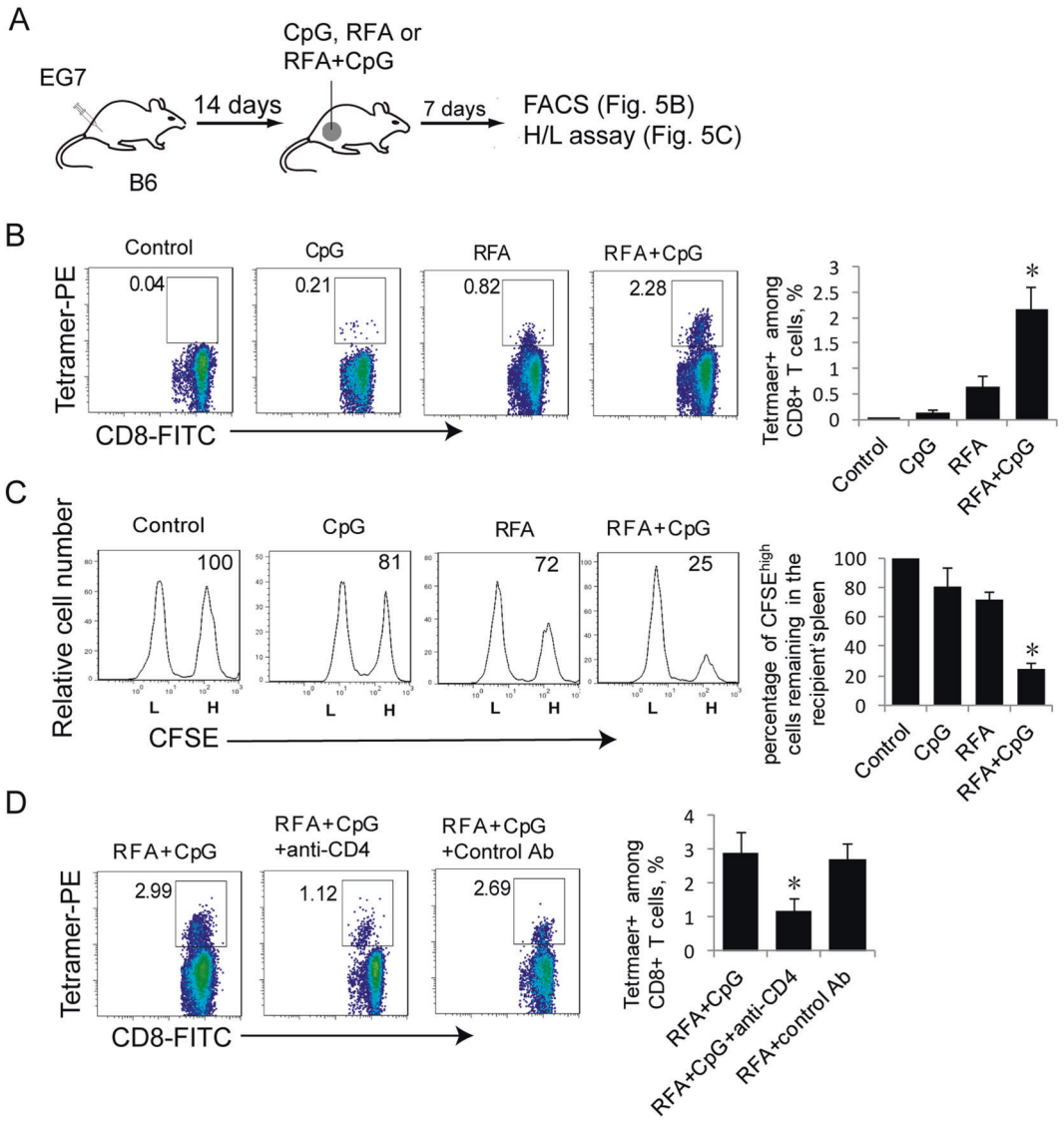

Fig. 5 CpG administration enhances RFA-induced CTL responses in vivo. **a** A diagram summarizing the design of RFA treatment experiments. **b** The cells in mouse blood samples derived from RFA/CpG-, RFA- or CpG-treated EG7 tumor-bearing mice (4 each group) were stained with OVA-specific PE-Tetramer and a FITC-labeled anti-CD8 antibody and analyzed by flow cytometry. The gating for OVA-specific CTLs stained with both the FITC-labeled anti-CD8 antibody and PE-tetramer from tumor-bearing mice treated with RFA, CpG or RFA+CpG was based on the assessment of CTLs in the control PBS-treated mice. A total of 20,000 $CD8^+$ T cells were counted. The value in each panel represents the percentage of OVA-specific $CD8^+$ T cells among the total $CD8^+$ T cell population. *$P < 0.05$ versus the cohort of RFA-activated $CD8^+$ T cells (Student's *t*-test). **c** In vivo cytotoxicity assay. The OVA-specific $CFSE^{high}$ (H) and control $CFSE^{low}$ (L) target cells remaining in the spleen of RFA/CpG- or RFA-treated tumor-bearing mice (4 each group) were analyzed by flow cytometry. The value in each panel represents the percentage of $CFSE^{high}$ target cells remaining in the recipient's spleen. *$P < 0.05$ versus the cohort of RFA-treated mice (Student's *t*-test). **d** The cells in mouse blood samples derived from RFA/CpG-treated EG7 tumor-bearing mice (4 each group) that underwent $CD4^+$ T-cell depletion were stained with OVA-specific PE-Tetramer and a FITC-labeled anti-CD8 antibody and analyzed by flow cytometry. The gating for OVA-specific CTLs stained with both the FITC-labeled anti-CD8 antibody and PE-tetramer from tumor-bearing mice immunized and treated with RFA and RFA +CpG was based upon the assessment of CTLs in the control PBS-treated mice. A total of 20,000 $CD8^+$ T cells were counted. The value in each panel represents the percentage of OVA-specific $CD8^+$ T cells among the total $CD8^+$ T-cell population. *$P < 0.05$ versus the cohort of the control antibody-treated mice (Student's *t*-test). One representative experiment out of two experiments is shown

and found that $CD8^+$ T-cell depletion and $CD4^+$ T-cell depletion abolished the RFA+CpG-induced inhibition of tumor growth, while NK cell depletion or control antibody treatment did not affect the RFA+CpG-induced inhibition of tumor growth (Fig. 6b). To further confirm the OVA-specific antitumor immune responses induced by the RFA+CpG treatment, we injected mice with EG7 tumor cells (4×10^6 and 2×10^6 cells) at two different sites (right and left sides of the lower back, respectively). When a right tumor reached ~350 mm^3, the corresponding left tumor was ~200 mm^3. We then performed the RFA+CpG treatment on the right tumor, and the mice were then monitored for tumor growth at both the RFA-treated right and the untreated left tumors (Fig. 6c). We demonstrated that the RFA+CpG treatment, but not RFA alone, resulted in significantly decreased growth of the left (distant) untreated tumors (Fig. 6c). To assess the ability of RFA-induced OVA-specific CTL responses to protect the mice from distant metastases, we i.v. challenged mice before RFA with $BL6\text{–}10_{OVA}$ melanoma cells, which efficiently form metastases in the lungs. The remaining RFA-treated EG7 tumors were surgically removed, and 20 days post $BL6\text{–}10_{OVA}$ tumor cell injection, the animals were

killed, and the lungs were collected (Fig. 6d). Remarkably, the RFA +CpG treatment significantly reduced lung tumor metastases compared to the RFA treatment alone (Fig. 6e, f). To assess the T-cell memory derived from the RFA-induced OVA-specific CTL responses, the RFA-treated tumors were surgically removed 7 days post RFA, and the mice received a DC_{OVA} boost 25 days post RFA. Memory $CD8^+$ T-cell recall responses were analyzed in the tail blood samples of boosted mice by flow cytometry. We demonstrated that OVA-specific $CD8^+$ T-cell recall responses in the RFA +CpG-treated mouse group (3.0%) were much higher than those in the RFA-treated mouse group (0.8%) (Fig. 6g). Therefore, our data indicate that the TLR9 agonist CpG enhances RFA-induced CTL responses, leading to: (i) potent inhibition of both primary RFA-treated tumor growth and distant untreated tumor growth, (ii) suppression of tumor metastases and (iii) enhancement of memory $CD8^+$ T-cell recall responses.

DISCUSSION

Apoptosis is a programmed cell death process that can be induced by many environmental stimuli, including irradiation and hyperthermia.[32] During early apoptosis responses, cell integrity remains relatively intact, and intracellular components are not released.[33] However, in the late apoptosis (necrosis) stage,[33] the cellular membrane becomes more permeable, leading to intracellular components being released into the surrounding tissue.[34] The intracellular components released from dying cells include some immunogenic molecules, such as RNA, DNA and HSPs.[35,36] Dying cells are removed by tissue-resident DCs in two stages. Dying tumor cells can attract DCs through the release of soluble "find-me" signals, such as nucleotides, and can also stimulate DCs to engulf apoptotic cells through their surface exposed "eat-me" signals, such as calreticulin and phosphatidylserine.[37] After performing phagocytosis, DCs differentiate into either immunogenic DCs, which express a large amount of MHCII and costimulatory CD40 and CD80 molecules, or tolerogenic DCs, which lack the expression of the above molecules but produce suppressive cytokines, such as IL-10, depending upon the specific immune components released from the dying tumor cells.[37]

Damage-associated molecular patterns released from dying cells, such as HSPs, can act on multiple pattern recognition receptors, inducing the activation and maturation of DCs.[35,36,38,39] The exposure time for the induction of tumor cell death by in vitro hyperthermia varied from tumor cell line to tumor cell line.[40,41] In this study, we selected 5 min for the exposure time because we found that 5 min was an optimal exposure time for maximal hyperthermia-induced EG7 tumor cell death at 45 °C and 65 °C. We demonstrate that, consistent with previous reports,[40,41] hyperthermia at 45 °C and 65 °C for 5 min induces tumor cell necrosis. Our experiments show that 65 °C hyperthermia not only induces more cell death but also upregulates intracellular HSP70 expression to a higher level compared to 45 °C hyperthermia. Furthermore, 65 °C-induced necrotic tumor cells were more immunogenic than 45 °C-induced cells, possibly due to the higher expression of HSP70, which is capable of activating both $CD4^+$ T cells and DCs and thus enhancing cross-priming $CD8^+$ T-cell responses.[35,36,38,39] DCs loaded with the protein lysate derived from in vivo RFA-ablated tumor tissues were previously reported to stimulate cytokine-induced killer cell responses.[42] We also reported that DCs that phagocytose irradiation-treated tumor cells induce potent anti-tumor CTL responses and immunity in animal models.[17] In this study, we showed that 65 °C-treated tumor cells trigger DC maturation and that DCs that phagocytose 65 °C-treated tumor cells stimulate more efficient OVA-specific CTL responses than DCs that phagocytose 45 °C-treated tumor cells.

RFA-induced $CD8^+$ CTL activity has primarily been measured by flow cytometry to detect nonspecific by monitoring the production of IFN-γ by $CD8^+$ T cells[7,43] and assessed by semiquantitative ELISPOT analysis to detect antigen-specific responses.[9–11] Recently, however, a few studies have reported accurate assessments of RFA-induced tumor-specific CTL responses using tumor antigen-specific PE-tetramer reagents.[44,45] In this study, we performed RFA therapy in our mouse model of OVA-expressing EG7 tumors, which allows a very accurate measurement of RFA-induced OVA-specific CTL responses by flow cytometry using PE-Tetramer and FITC-labeled anti-CD8 antibody staining. We demonstrated that RFA (65 °C) treatment can stimulate OVA-specific $CD8^+$ T-cell responses capable of killing OVA-specific target cells in vivo. By daily tumor monitoring, we demonstrated that RFA (65 °C) treatment completely abolishes small EG7 tumors. Since RFA is often used in the clinical setting to treat unresectable tumors, we also performed RFA (65 °C) treatment on larger EG7 tumors. This therapeutic strategy of RFA administration at only the central site of a larger tumor produced no significant reduction in tumor growth, although RFA-treated tumors showed slightly slower growth in the first 6 days post RFA therapy compared to untreated tumors, which is consistent with the results of a recent clinical RFA report on stage IV melanoma,[44] which suggests that a strategy of multiple RFA treatments at different areas in larger tumors may potentially produce better outcomes.

TLR9 agonistic oligonucleotides containing CpG are well known to promote $CD4^+$ T helper type 1 (Th1) cell and CTL responses through binding to endosomal TLR9,[21,22] which leads to IL-12 induction via the activation of TLR9 signaling.[46] Consistent with this, CpG has been used to improve the efficacy of various cancer immunotherapy strategies. These include use of CpG in vaccination,[47] local low-dose radiation therapy[48] and programmed cell death protein-1 (PD-1) blockade.[49] In this study, we examined the effect of intratumoral CpG on antitumor RFA therapy and assessed whether $CD4^+$ and $CD8^+$ T cells and NK cells are required for the antitumor immunity derived from RFA+CpG therapy. We demonstrated that CpG+RFA treatment results in potent $CD4^+$ T cell-dependent CTL responses that lead to the significant inhibition of tumor growth. However, NK cells are not involved in CpG+RFA-induced inhibition of tumor growth. Intratumoral tumor-associated DCs were previously found to exhibit defective tumor antigen cross-presentation to T cells and defective T-cell proliferation stimulation.[50] Recently, two types of tumor-associated DCs (tolerogenic $CD11c^+CD11b^+$ DC1 and immunogenic $CD11c^+CD103^+$ DC2) were defined.[28] The latter represent active antigen-presenting cells in the tumor microenvironment that exhibit unique antigen processing and presentation capabilities and are superior stimulators of CTL responses.[28] Our data reveal that intratumoral administration of CpG expands the population of tumor-associated immunogenic $CD11c^+CD103^+$ DC2, leading to more efficient DC stimulation of intratumoral T-cell proliferation. Two types of tumor-associated macrophages (inflammatory $CD11b^+F4/80^+MHCII^+$ M1 and tolerogenic $CD11b^+F4/80^+MHCII^-$M2) were previously defined.[29] Tumor-associated M1 cells can significantly halt tumor growth,[51,52] secrete inflammatory cytokines (IFN-γ and IL-12) that drive the polarization of Th1 cells, produce chemokines (CXCL9 and CXCL10) that recruit T cells into tumors and suppress tumor-associated M2 cell development,[53,54] while M2 cells promote tumor angiogenesis and growth and secrete the tolerogenic cytokine IL-10 to induce immune suppression.[55] Our data revealed that the intratumoral administration of CpG increases the frequency of tumor-associated immunogenic $CD11b^+F4/80^+MHCII^+$ M1 cells but reduces the frequency of tolerogenic $CD11b^+F4/80^+MHCII^-$M2 cells as well as enhances $CD4^+$ and $CD8^+$ T-cell tumor infiltration, thus resulting in the potent inhibition of primary RFA-treated or distant untreated tumor growth and a significant reduction in lung metastasis. Metabolic programming is crucial for immune cell development and

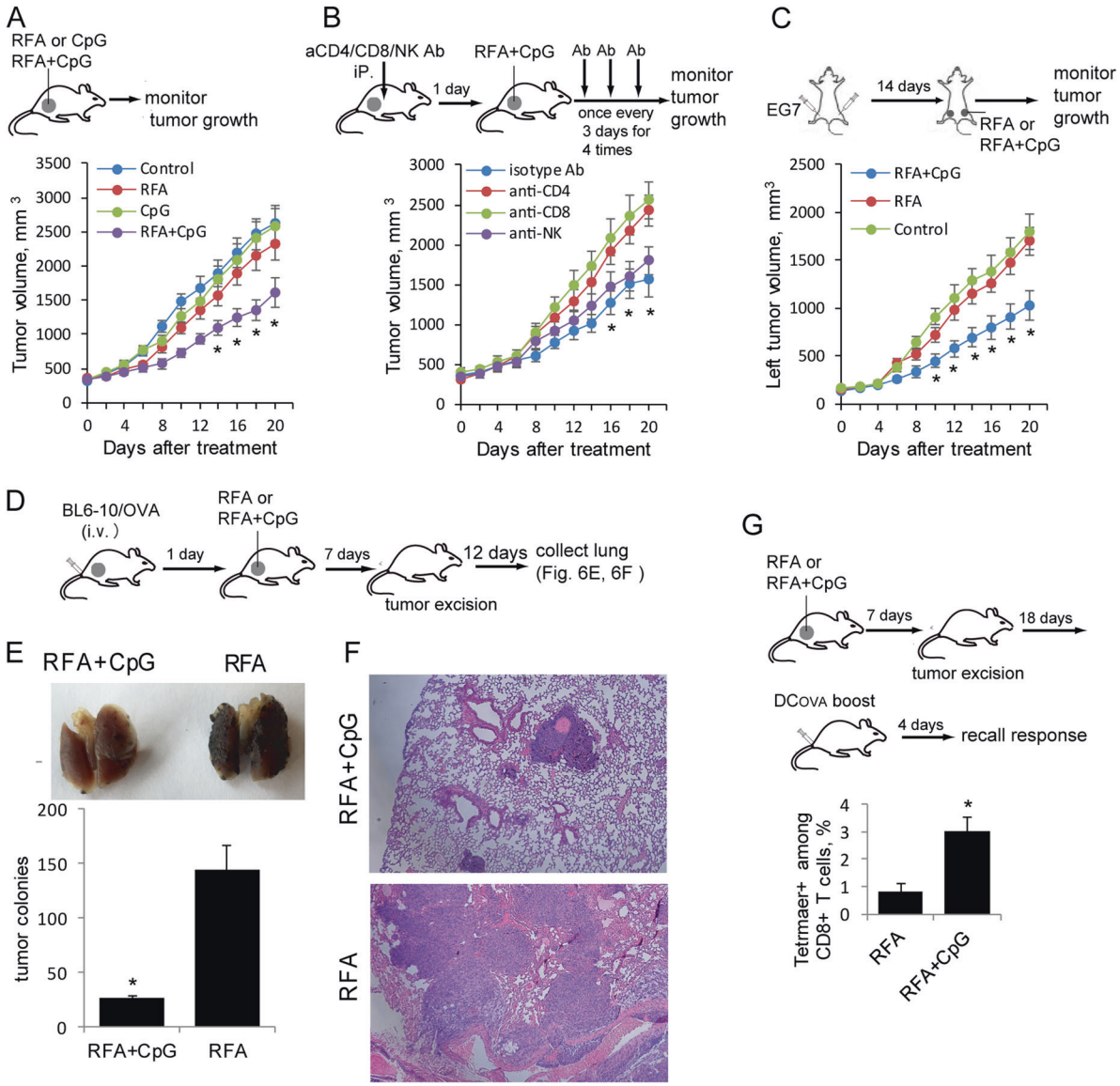

Fig. 6 Combination treatment with RFA and CpG leads to the inhibition of larger tumor growth and lung tumor metastasis. **a** A schematic diagram of the RFA, CpG and RFA+CpG treatments for mice bearing larger EG7 tumors. Mice bearing larger EG7 tumors(8 per group) were treated with RFA, CpG, RFA+CpG or the control PBS. Tumor growth or regression was monitored. *$P < 0.05$ versus the cohort of the control or CpG-treated mice (Student's *t*-test). **b** Experimental setup of the RFA+CpG treatment of mice bearing larger EG7 tumors with or without the depletion of $CD4^+$ T, $CD8^+$ T and NK cells. To assess the involvement of $CD4^+$ T, $CD8^+$ T and NK cells in the RFA+CpG-induced inhibition of tumor growth, mice bearing larger EG7 tumors (8 per group) were injected with anti-CD4, anti-CD8 or anti-NK Abs for the depletion of $CD4^+$ or $CD8^+$ T cells or NK cells, respectively. Mice were then treated with RFA+CpG therapy one day after the antibody injection. The antibody injection was repeated once every 3 days for a total of 4 injections. Tumor growth or regression was monitored. *$P < 0.05$ versus the cohort of $CD4^+$ or $CD8^+$ T cell-depleted mice (Student's *t*-test). **c** C57BL/6 mice were injected subcutaneously with EG7 cells (2×10^6 and 4×10^6) on the left and right sides of the lower back, respectively. When the right and left tumors reached ~350 mm^3 and ~200 mm^3, respectively, RFA+CpG or RFA treatment was performed on only the right tumor. The growth of the left and right site tumors was monitored. For ethical reasons, mice were killed when the right site tumor reached ~2500 mm^3. The sizes of the left untreated tumors in the different groups were compared. *$P <$ 0.05 versus the cohort of untreated control mice. **d** A schematic diagram of the experiments assessing the antimetastatic activity of the RFA +CpG treatment in mice bearing larger tumors. Mice with larger s.c. EG7 tumors (8 per group) were i.v. injected with $BL6–10_{OVA}$ cells. One day later, RFA or RFA+CpG was performed. The s.c. tumors were surgically removed 7 days post RFA therapy. The mice were killed 20 days post $BL6–10_{OVA}$ cell injection, and the lungs were collected. **e** Metastatic black $BL6–10_{OVA}$ tumor colonies in the lungs of the mice (5 per group) were counted. *$P < 0.05$ versus the cohort of RFA-treated mice (Student's *t*-test). **f** The lungs were sectioned and stained with hematoxylin and eosin. **g** A schematic diagram of the experiments assessing the memory T cells produced by RFA+CpG treatment in mice bearing large tumors. Mice bearing larger s.c. EG7 tumors (6 per group) were treated with RFA or RFA+CpG. The tumors were surgically removed 7 days post RFA therapy. Mice were boosted with DC_{OVA} 25 days post RFA therapy, and the memory T-cell recall responses were assessed 4 days after the boost by flow cytometry. *$P < 0.05$ versus the cohort of RFA-treated mice (Student's *t*-test). One representative experiment out of two experiments is shown

functions.[56] It has been demonstrated that (i) immunogenic and tolerogenic immune cells have different metabolic profiles. Immunogenic DCs and M1 mainly rely on glycolysis for energy, whereas tolerogenic DCs and M2 are supported by mitochondrial fatty-acid oxidation (FAO) for adenosine triphosphate production, and (ii) TLR stimulation signals control metabolic programming and glycolysis via the activation of the AKT–mTORC1–HIF-1α pathway.[56] Therefore, the conversion of tolerogenic DC1 and M2 into immunogenic DC2 and M1 by CpG through the activation of the AKT–mTORC1 pathway,[57] as observed in this study, is possibly derived from the CpG-mediated metabolic switch from FAO to glycolysis.

To improve the therapeutic effects of RFA for cancer treatment, various combinational therapies have been reported.[8,46,58] These approaches include combinations with PD-1 blockade,[8] vaccination with heat-shocked tumor cell lysate-pulsed DCs[58] and intratumoral injection of DCs[46] post RFA. Recently, Ferrara and colleagues[43,45] performed a combinational RFA therapy with CpG administration and PD-1 blockade in animal tumor models and demonstrated a critical role of CpG administration/PD-1 blockade-induced priming prior to RFA therapy in the stimulation of highly effective systemic immune responses leading to greatly improved efficacy in RFA-mediated cancer therapy.

Various TLR agonists have also been found to act as effective adjuvants for vaccines.[59] For example, the intratumoral administration of a TLR9 agonist alone induced tumor-specific $CD8^+$ T-cell responses,[60] and the injection of a TLR3 or TLR9 agonist significantly enhanced adaptive T cell-based cancer therapy.[61] The intratumoral delivery of TLR7 or TLR9 agonists in combination with cancer radiotherapy has been found to give rise to systemic immune effects on nonirradiated tumor lesions.[62,63] In this study, we demonstrated that a TLR9 agonist enhances RFA-induced tumor-specific CTL responses, leading to the potent inhibition of not only tumor growth but also lung metastasis. The establishment of an optimal protocol for RFA cancer therapy in combination with the TLR9 agonist CpG and other TLR agonists, such as the TLR3 agonist polyinosinic:polycytidylic acid, TLR4 agonist lipopolysaccharide and TLR7 agonist U-rich ssRNA, is being actively pursued in our laboratory by using our in vivo OVA-specific tumor model.

Taken together, our data indicate that TLR9 activation enhances radiofrequency ablation-induced CTL responses which, in turn, leads to the potent inhibition of tumor growth and distant metastasis. Therefore, the application of TLR agonists may represent a promising treatment strategy to improve the outcomes of RFA cancer therapy and support the survival of cancer patients.

ACKNOWLEDGEMENTS

This work was supported by grants from CoMRAD (#417578), College of Medicine, University of Saskatchewan, Prostate Cancer Fight Foundation (#417782), Royal University Hospital Research Foundation (#417450) and Saskatchewan Health Research Foundation (#418672).

ADDITIONAL INFORMATION

Competing interests: The authors declare no competing interests.

Publisher's note: Springer Nature remains neutral with regard to jurisdictional claims in published maps and institutional affiliations.

REFERENCES

1. Wust, P. et al. Hyperthermia in combined treatment of cancer. *Lancet Oncol.* **3**, 487–497 (2002).
2. Lencioni, R. et al. Early-stage hepatocellular carcinoma in patients with cirrhosis: long-term results of percutaneous image-guided radiofrequency ablation. *Radiology* **234**, 961–967 (2005).
3. Gillams, A. & Lees, W. Five-year survival in 309 patients with colorectal liver metastases treated with radiofrequency ablation. *Eur. Radiol.* **19**, 1206–1213 (2009).
4. Zemlyak, A., Moore, W. H. & Bilfinger, T. V. Comparison of survival after sublobar resections and ablative therapies for stage I non-small cell lung cancer. *J. Am. Coll. Surg.* **211**, 68–72 (2010).
5. Chu, K. F. & Dupuy, D. E. Thermal ablation of tumours: biological mechanisms and advances in therapy. *Nat. Rev. Cancer* **14**, 199–208 (2014).
6. Williams, M. A. & Bevan, M. J. Effector and memory CTL differentiation. *Annu Rev. Immunol.* **25**, 171–192 (2007).
7. Wissniowski, T. T. et al. Activation of tumor-specific T lymphocytes by radiofrequency ablation of the VX2 hepatoma in rabbits. *Cancer Res.* **63**, 6496–6500 (2003).
8. Shi, L. et al. PD-1 blockade boosts radiofrequency ablation-elicited adaptive immune responses against tumor. *Clin. Cancer Res.* **22**, 1173–1184 (2016).
9. Zerbini, A. et al. Radiofrequency thermal ablation of hepatocellular carcinoma liver nodules can activate and enhance tumor-specific T-cell responses. *Cancer Res.* **66**, 1139–1146 (2006).
10. Napoletano, C. et al. RFA strongly modulates the immune system and anti-tumor immune responses in metastatic liver patients. *Int J. Oncol.* **32**, 481–490 (2008).
11. Widenmeyer, M. et al. Analysis of tumor antigen-specific T cells and antibodies in cancer patients treated with radiofrequency ablation. *Int J. Cancer* **128**, 2653–2662 (2011).
12. Sims, S., Willberg, C. & Klenerman, P. MHC-peptide tetramers for the analysis of antigen-specific T cells. *Expert Rev. Vaccin.* **9**, 765–774 (2010).
13. Albert, M. L., Sauter, B. & Bhardwaj, N. Dendritic cells acquire antigen from apoptotic cells and induce class I-restricted CTLs. *Nature* **392**, 86–89 (1998).
14. Goldszmid, R. S. et al. Dendritic cells charged with apoptotic tumor cells induce long-lived protective CD4+and CD8+T cell immunity against B16 melanoma. *J. Immunol.* **171**, 5940–5947 (2003).
15. Inzkirweli, N. et al. Antigen loading of dendritic cells with apoptotic tumor cell-preparations is superior to that using necrotic cells or tumor lysates. *Anticancer Res.* **27**, 2121–2129 (2007).
16. Chen, Z. et al. Efficient antitumor immunity derived from maturation of dendritic cells that had phagocytosed apoptotic/necrotic tumor cells. *Int J. Cancer* **93**, 539–548 (2001).
17. Parameswaran, S., Khalil, M., Ahmed, K. A., Sharma, R. K. & Xiang, J. Enhanced protective immunity derived from dendritic cells with phagocytosis of CD40 ligand transgene-engineered apoptotic tumor cells via increased dendritic cell maturation. *Tumori* **101**, 637–643 (2015).
18. Zhang, B. et al. Study of the relationship between the target tissue necrosis volume and the target tissue size in liver tumours using two-compartment finite element RFA modelling. *Int J. Hyperthermia* **30**, 593–602 (2014).
19. Zhang, B., Moser, M. A., Luo, Y., Zhang, E. M. & Zhang, W. Evaluation of the current radiofrequency ablation systems using axiomatic design theory. *Proc. Inst. Mech. Eng. H* **228**, 397–408 (2014).
20. Erez, A. & Shitzer, A. Controlled destruction and temperature distributions in biological tissues subjected to monoactive electrocoagulation. *J. Biomech. Eng.* **102**, 42–49 (1980).
21. Hemmi, H. et al. A Toll-like receptor recognizes bacterial DNA. *Nature* **408**, 740–745 (2000).
22. Zhang, X., Munegowda, M. A., Yuan, J., Wei, Y. & Xiang, J. Optimal TLR9 signal converts tolerogenic CD4–8–DCs into immunogenic ones capable of stimulating antitumor immunity via activating CD4+Th1/Th17 and NK cell responses. *J. Leukoc. Biol.* **88**, 393–403 (2010).
23. Xie, Y. F. et al. A novel T cell-based vaccine capable of stimulating long-term functional CTL memory against B16 melanoma via CD40L signaling. *Cell Mol. Immunol.* **10**, 72–77 (2013).
24. Zhang, B., Moser, M. A., Zhang, E. M., Luo, Y. & Zhang, W. Numerical analysis of the relationship between the area of target tissue necrosis and the size of target tissue in liver tumours with pulsed radiofrequency ablation. *Int J. Hyperthermia* **31**, 715–725 (2015).
25. Umeshappa, C. S. et al. Innate and adoptive immune cells contribute to natural resistance to systemic metastasis of B16 melanoma. *Cancer Biother Radiopharm.* **30**, 72–78 (2015).
26. Xu, A., Zhang, L., Chen, Y., Lin, Z. & Li, R. Immunogenicity and efficacy of a rationally designed vaccine against vascular endothelial growth factor in mouse solid tumor models. *Cancer Immunol. Immunother.* **66**, 181–192 (2017).
27. Wang, R. et al. Novel exosome-targeted T-cell-based vaccine counteracts T-cell anergy and converts CTL exhaustion in chronic infection via CD40L signaling through the mTORC1 pathway. *Cell Mol. Immunol.* **14**, 529–545 (2017).
28. Broz, M. L. et al. Dissecting the tumor myeloid compartment reveals rare activating antigen-presenting cells critical for T cell immunity. *Cancer Cell* **26**, 638–652 (2014).

29. Soncin, I. et al. The tumour microenvironment creates a niche for the self-renewal of tumour-promoting macrophages in colon adenoma. *Nat. Commun.* **9**, 582 (2018).
30. Liu, Y. & Cao, X. Intratumoral dendritic cells in the anti-tumor immune response. *Cell Mol. Immunol.* **12**, 387–390 (2015).
31. Itano, A. A. et al. Distinct dendritic cell populations sequentially present antigen to CD4 T cells and stimulate different aspects of cell-mediated immunity. *Immunity* **19**, 47–57 (2003).
32. Kerr, J. F., Wyllie, A. H. & Currie, A. R. Apoptosis: a basic biological phenomenon with wide-ranging implications in tissue kinetics. *Br. J. Cancer* **26**, 239–257 (1972).
33. Woo, M., Hakem, R. & Mak, T. W. Executionary pathway for apoptosis: lessons from mutant mice. *Cell Res.* **10**, 267–278 (2000).
34. Krysko, D. V., D'Herde, K. & Vandenabeele, P. Clearance of apoptotic and necrotic cells and its immunological consequences. *Apoptosis* **11**, 1709–1726 (2006).
35. Xie, Y. et al. Membrane-bound HSP70-engineered myeloma cell-derived exosomes stimulate more efficient CD8(+) CTL- and NK-mediated antitumour immunity than exosomes released from heat-shocked tumour cells expressing cytoplasmic HSP70. *J. Cell Mol. Med.* **14**, 2655–2666 (2010).
36. Figueiredo, C. et al. Heat shock protein 70 (HSP70) induces cytotoxicity of T-helper cells. *Blood* **113**, 3008–3016 (2009).
37. Poon, I. K. H., Hulett, M. D. & Parish, C. R. Molecular mechanisms of late apoptotic/necrotic cell clearance. *Cell Death Differ.* **17**, 381–397 (2010).
38. Shi, H. et al. Hyperthermia enhances CTL cross-priming. *J. Immunol.* **176**, 2134–2141 (2006).
39. Yang, D. et al. High mobility group box-1 protein induces the migration and activation of human dendritic cells and acts as an alarmin. *J. Leukoc. Biol.* **81**, 59–66 (2007).
40. Vorotnikova, E., Ivkov, R., Foreman, A., Tries, M. & Braunhut, S. J. The magnitude and time-dependence of the apoptotic response of normal and malignant cells subjected to ionizing radiation versus hyperthermia. *Int J. Radiat. Biol.* **82**, 549–559 (2006).
41. Garcia, M. P., Cavalheiro, J. R. & Fernandes, M. H. Acute and long-term effects of hyperthermia in B16-F10 melanoma cells. *PLoS ONE* **7**, e35489 (2012).
42. Shan, C. C. et al. Cytokine-induced killer cells co-cultured with dendritic cells loaded with the protein lysate produced by radiofrequency ablation induce a specific antitumor response. *Oncol. Lett.* **9**, 1549–1556 (2015).
43. Silvestrini, M. T. et al. Priming is key to effective incorporation of image-guided thermal ablation into immunotherapy protocols. *JCI Insight* **2**, e90521 (2017).
44. Domingo-Musibay, E. et al. Endogenous heat-shock protein induction with or without radiofrequency ablation or cryoablation in patients with stage IV melanoma. *Oncologist* **22**, 1026–e1093 (2017).
45. Chavez, M. et al. Distinct immune signatures in directly treated and distant tumors result from TLR adjuvants and focal ablation. *Theranostics* **8**, 3611–3628 (2018).
46. Dromi, S. A. et al. Radiofrequency ablation induces antigen-presenting cell infiltration and amplification of weak tumor-induced immunity. *Radiology* **251**, 58–66 (2009).
47. Pulendran, B. Modulating vaccine responses with dendritic cells and Toll-like receptors. *Immunol. Rev.* **199**, 227–250 (2004).
48. Frank, M. J. et al. In situ vaccination with a TLR9 agonist and local low-dose radiation induces systemic responses in untreated indolent lymphoma. *Cancer Discov.* **8**, 1258–1269 (2018).
49. Ribas, A. et al. SD-101 in combination with pembrolizumab in advanced melanoma: results of a phase Ib, multicenter study. *Cancer Discov.* **8**, 1250–1257 (2018).
50. McDonnell, A. M. et al. Tumor-infiltrating dendritic cells exhibit defective cross-presentation of tumor antigens, but is reversed by chemotherapy. *Eur. J. Immunol.* **45**, 49–59 (2015).
51. Colombo, M. P. & Mantovani, A. Targeting myelomonocytic cells to revert inflammation-dependent cancer promotion. *Cancer Res.* **65**, 9113–9116 (2005).
52. Zeisberger, S. M. et al. Clodronate-liposome-mediated depletion of tumour-associated macrophages: a new and highly effective antiangiogenic therapy approach. *Br. J. Cancer* **95**, 272–281 (2006).
53. Mantovani, A. et al. The chemokine system in diverse forms of macrophage activation and polarization. *Trends Immunol.* **25**, 677–686 (2004).
54. Murray, P. J. & Wynn, T. A. Protective and pathogenic functions of macrophage subsets. *Nat. Rev. Immunol.* **11**, 723–737 (2011).
55. Chanmee, T., Ontong, P., Konno, K. & Itano, N. Tumor-associated macrophages as major players in the tumor microenvironment. *Cancers* **6**, 1670–1690 (2014).
56. Huang, L., Xu, H. & Peng, G. TLR-mediated metabolic reprogramming in the tumor microenvironment: potential novel strategies for cancer immunotherapy. *Cell Mol. Immunol.* **15**, 428–437 (2018).
57. Ma, C., Spies, N.P., Gong, T., Jones, C.X. & Chu, W.M. Involvement of DNA-PKcs in the type I IFN response to CpG-ODNs in conventional dendritic cells in TLR9-dependent or -independent manners. *PLoS One*. 10, e0121371 (2015).
58. Liu, Q. et al. Abrogation of local cancer recurrence after radiofrequency ablation by dendritic cell-based hyperthermic tumor vaccine. *Mol. Ther.* **17**, 2049–2057 (2009).
59. Reed, S. G., Bertholet, S., Coler, R. N. & Friede, M. New horizons in adjuvants for vaccine development. *Trends Immunol.* **30**, 23–32 (2009).
60. Amos, S. M. et al. Adoptive immunotherapy combined with intratumoral TLR agonist delivery eradicates established melanoma in mice. *Cancer Immunol. Immunother.* **60**, 671–683 (2011).
61. Molenkamp, B. G. et al. Local administration of PF-3512676 CpG-B instigates tumor-specific CD8+T-cell reactivity in melanoma patients. *Clin. Cancer Res*. **14**, 4532–4542 (2008).
62. Dewan, M. Z. et al. Synergy of topical toll-like receptor 7 agonist with radiation and low-dose cyclophosphamide in a mouse model of cutaneous breast cancer. *Clin. Cancer Res.* **18**, 6668–6678 (2012).
63. Adams, S. et al. Topical TLR7 agonist imiquimod can induce immune-mediated rejection of skin metastases in patients with breast cancer. *Clin. Cancer Res* **18**, 6748–6757 (2012).